Complete Assignment of the Aromatic Proton Magnetic Resonance Spectrum of the Kringle 1 Domain from Human Plasminogen: Structure of the Ligand-Binding Site†

Andrea Motta,‡,§ Richard A. Laursen,∥ Miguel Llinás,*,‡ Alexander Tulinsky,⊥ and Chang H. Park⊥

Department of Chemistry, Carnegie-Mellon University, Pittsburgh, Pennsylvania 15213, Department of Chemistry, Boston University, Boston, Massachusetts 02215, and Department of Chemistry, Michigan State University, East Lansing, Michigan 44824

Received December 4, 1986; Revised Manuscript Received February 25, 1987

ABSTRACT: The kringle 1 domain of human plasminogen has been investigated by ^{1}H NMR spectroscopy at 300 and 600 MHz on the basis of a fragment obtained via controlled proteolysis of the zymogen with *Staphylococcus aureus V8* protease. The aromatic spectrum has been fully analyzed and all resonances assigned. The Tyr ring signals were identified by reference to the recently reported spectra of the plasminogen kringle 4 homologues from human, bovine, and porcine origin [Ramesh, V., Gyenes, M., Patthy, L., & Llinás, M. (1986) *Eur. J. Biochem. 159*, 581–595]. In particular, Tyr^{74} was assigned on the basis of a proton Overhauser experiment showing cross-relaxation with the Trp-II (Trp^{62}) indole ring, a connectivity previously observed in all the kringle 4 variants and that clearly represents a conserved feature of the kringle structure. Ligand binding was investigated by monitoring the effects of the antifibrinolytic drugs ϵ-aminohexanoic acid and *p*-benzylaminesulfonic acid (BASA) on the ^{1}H NMR spectrum of kringle 1. It is observed that although most aromatic resonances are perturbed by ligand presence, the chemical shift response is significantly more marked for Phe^{36}, Trp^{62}, and Tyr^{72}. Proton Overhauser experiments centered on aromatic transitions from these residues reveal efficient cross-relaxation with BASA, which indicates direct contacts between the hydrophobic side chain rings and the ligand hydrocarbon moiety at the binding site. A close interaction is also found between Tyr^{64} and Try^{72} which indicates that the residue 64 ring is positioned close to the binding site. Excellent overall agreement is found between the NMR data and the molecular folding of the prothrombin kringle 1 determined crystallographically [Park, C. H., & Tulinsky, A. (1986) *Biochemistry 25*, 3977–3982]. A structure is proposed here for the kringle 1 lysine-binding site which is based upon the NMR results, the X-ray structure, and computer graphics modeling. It is concluded that although features of the lysine-binding site are common to plasminogen kringles 1 and 4, in kringle 1 the binding site extends beyond the kringle inner loop as it encompasses residues Arg^{34} and Phe^{36} as well. Furthermore, it appears that in kringle 1 Arg^{34} and Asp^{55} are likely to play a direct role in the ligand–kringle 1 interaction by reinforcing the polarity of the cationic and anionic centers of the side chains of Arg^{71} and Asp^{57}, which have been implicated to provide the electrostatic charges in kringle 4 that balance those of the ligand dipole at the binding site.

Plasminogen contains a tandem array of five homologous modules of M_r ~10000 each, known as "kringles" (Sottrup-Jensen et al., 1978), whose principal role appears to be the anchoring of the enzyme plasmin to its main target substrate, the fibrin matrix of blood clots (Thorsen et al., 1981). Kringles are also thought to mediate the interaction of the protein with the inhibitor α_2-antiplasmin (Wiman et al., 1979; Thorsen et al., 1981). Among the plasminogen kringles, kringle 1 is likely to fulfill a key role in determining the plasminogen mode of action since it is known to carry a fibrin-binding site (Vâli & Patthy, 1984) as well as a lysine-binding site (Lerch et al., 1980; De Marco et al., 1982), postulated to afford a mechanism for the attachment to plasmin substrates. Furthermore, as shown by Rickli and co-workers (Lerch et al., 1980), kringle 1 efficiently binds the plasminogen activation peptide, a potential effector of activity. In order to better understand the molecular biochemistry of plasmin(ogen), it thus appears important to clarify both the structure and the mode of action of kringle domains, most particularly of kringle 1.

Chart I: Kringle Ligands

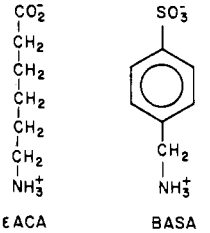

From ^{1}H NMR ligand perturbation studies and protein-ligand saturation transfer (Overhauser) experiments on kringle 4, we have learned that Trp-II (Trp^{62}?), Phe^{64}, and Trp^{72} are at the lysine-binding site and that Tyr^{74} is in contact with Trp-II (Llinás et al., 1985; De Marco et al., 1986). Our working model has been one in which the aromatic side chains provide lipophilic contact surfaces that interact with the hydrocarbon moiety of the ligand molecule, whose polar end groups form ion pairs with acidic and basic residues, such as Asp^{57} and Arg^{71} (Trexler et al., 1982), within the kringle inner

† This research was supported by the U.S. Public Health Service, NIH Grants HL 15535, HL 25942, and HL 29409. The 600-MHz NMR facility is supported by NIH Grant RR 00292.

‡ Carnegie-Mellon University.

§ Permanent address: Istituto per la Chimica di Molecole di Interesse Biologico, Consiglio Nazionale delle Ricerche, 80072 Arco Felice, Napoli, Italy.

∥ Boston University.

⊥ Michigan State University.

0006-2960/87/0426-3827$01.50/0 © 1987 American Chemical Society

loop. It is thus important to establish how general the validity of this model is and whether it applies to kringle 1 as well. The perturbation of the kringle 1 Tyr^{72} (which substitutes for Trp^{72} in kringle 4) aromatic spectrum by *p*-benzylaminesulfonic acid (BASA)[1] hinted that such may be the case (De Marco et al., 1982). To approach the problem, one must first assign all of the resonances in the kringle 1 aromatic spectrum which, thus far, has only been unambiguously analyzed in terms of the individual His and Trp spin systems for the kringle in the presence of the ligand εACA (Motta et al., 1986) (Chart I).

In this paper, we reexamine the kringle 1 aromatic spectrum and derive assignments of the phenol and phenyl ring resonances observed in a kringle 1 domain fragment obtained via *Staphylococcus aureus* V8 protease treatment of the kringle 1 + 2 + 3 fragment (Motta et al., 1986), which releases the first kringle by cleavage at the Glu^{81}-Glu^{82}-Glu^{83} tripeptide segment, i.e., without introducing spurious aromatic groups from the neighbor kringle 2 module (Vâli & Patthy, 1984). We also report proton Overhauser experiments indicating that, in conjunction with Tyr^{72}, both Trp^{62} and Phe^{36} directly participate in ligand binding. Involvement of the latter aromatic ring is important as it implies that, in contrast to what is known for kringle 4, the binding site in kringle 1 is also structured by residues outside the kringle inner loop. The NMR results are correlated with the three-dimensional structure of kringle 1 of prothrombin (Park & Tulinsky, 1986), modified by computer graphics modeling to correspond to the kringle 1 sequence of plasminogen, and then modulated by NMR constraints to generate a three-dimensional approximation of the lysine-binding region.

Materials and Methods

Kringle 1 samples were obtained by *Staphylococcus aureus* V8 protease digestion of the human plasminogen kringle 1 + 2 + 3 fragment, as previously reported (Motta et al., 1986). Protein solutions for NMR studies were (0.5–1.0) × 10^{-3} M in ^2H_2O, the solvent originating from Merck Sharp & Dohme Inc. of Canada. BASA belonged to a batch described elsewhere (Hochschwender et al., 1983), and εACA was purchased from Sigma Chemical Co., St. Louis, MO. 1D ^1H NMR spectra were recorded at 300 MHz using a Bruker WM-300 instrument, and at 600 MHz with the spectrometer of the NIH National NMR Facility for Biomedical Studies at Carnegie-Mellon University. All spectra were acquired in the Fourier mode with quadrature detection. Resolution enhancement was achieved by Gaussian convolution (Ernst, 1966; Ferrige & Lindon, 1978). Chemical shifts are referred to a sodium 3-(trimethylsilyl)[2,2,3,3-$^2H_4$]propionate signal, using dioxane as the internal reference standard (De Marco, 1977).

COSY (Wider et al., 1984) spectra were obtained from 512 measurements with t_1 values scaled from 320 μs to 168 ms, adding 320 transients for eact t_1 setting, using a spectral width of 3448 Hz and 2048 data points to store the data, which yields a digital resolution of 3.4 Hz along both dimensions. The residual $^1H^2HO$ signal was irradiated in the gated mode for 1.2 s, and the system was allowed to relax for 1.2 s. Proper phase cycling was selected to yield N-type peaks (Bruker Aspect 2000 data package). Before Fourier transformation, the time domain data matrix was multiplied with a sine bell, or an 18°-shifted sine function, in both dimensions. COSY spectra, unless stated otherwise, are reported as symmetrized contour plots in the absolute value mode.

Transient (Gordon & Wüthrich, 1978; Szeverenyi et al., 1980) and truncated (Dubs et al., 1979) Overhauser experiments were performed as described in the corresponding figure captions, and are reported as difference (unperturbed minus perturbed) spectra; thus, negative NOEs appear with a positive sign.

Computer graphics modeling was carried out on an Evans & Sutherland TS-350 system with FRODO (Jones, 1982).

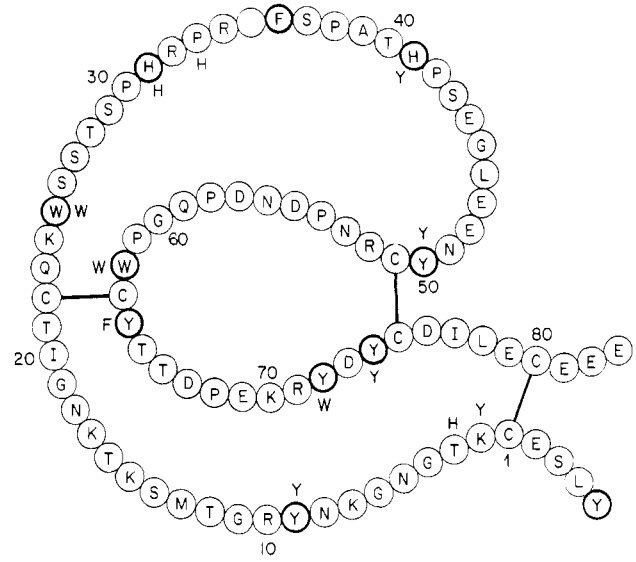

FIGURE 1: Outline of the kringle 1 structure. The numbering of amino acid residues starts from the half-cystine closest to the N-terminus (Sottrup-Jensen et al., 1978; Lerch et al., 1980). The aromatic amino acids found in human plasminogen kringle 1 and kringle 4 are indicated within heavy trace circles (kringle 1) or adjoining the structure (kringle 4), using the conventional one-letter code. Deletions have been introduced at sites 35 (kringle 1 and kringle 4) and 59 (kringle 4) in order to facilitate comparison with homologous domains.

Results

Aromatic amino acids in the kringle 1 and kringle 4 sequences are shown in Figure 1. A high degree of aromatic conservancy is indicated for the two kringles: about 50% of the aromatic rings are identically located in the two domains with the extent of homology increasing to ~78% when aromatic–aromatic substitutions are considered (His → Tyr, Tyr → Phe, and Tyr → Trp, at sites 41, 64, and 72, respectively). This suggests an important role for aromatic residues in determining the kringle folding and/or function.

Histidines and Tryptophans. Kringle 1 contains two His residues located at sites 31 and 41 and two Trp residues at sites 25 and 62 (Figure 1). The complete aromatic region 1D spectra and the corresponding COSY spectra of kringle 1 at 300 MHz are depicted in Figure 2A and Figure 2B, respectively. Cross-peaks due to coupling between the imidazole H2 and the H4 of His-I (peaks 4 and 2) and of His-II (peaks 3 and 6) can readily be observed in the COSY spectrum, confirming the ring proton pairings derived from pH titration studies on a sample containing the ligand εACA (Motta et al., 1986). We have previously also established that the His-II H4 resonates at lower field positions relative to the H2 signal (H-II, Figure 2A). Such "reverse" ordering is also observed for a pair of His singlets in kringle 4 (Llinás et al., 1983; De Marco et al., 1985b). Since on going from kringle 1 to kringle 4, His^{31} is the only His residue which is conserved (Figure 1), His-II has been assigned to His^{31} and, by exclusion, His-I to His^{41} (Llinás et al., 1983; Motta et al., 1986).

[1] Abbreviations: BASA, *p*-benzylaminesulfonic acid; COSY, two-dimensional chemical shift correlated spectroscopy; εACA, ε-aminocaproic acid (6-aminohexanoic acid); K1, kringle 1; K4, kringle 4; NOE, nuclear Overhauser effect; pH*, glass electrode pH reading uncorrected for deuterium isotope effect; 1D, one dimensional; 2D, two dimensional.

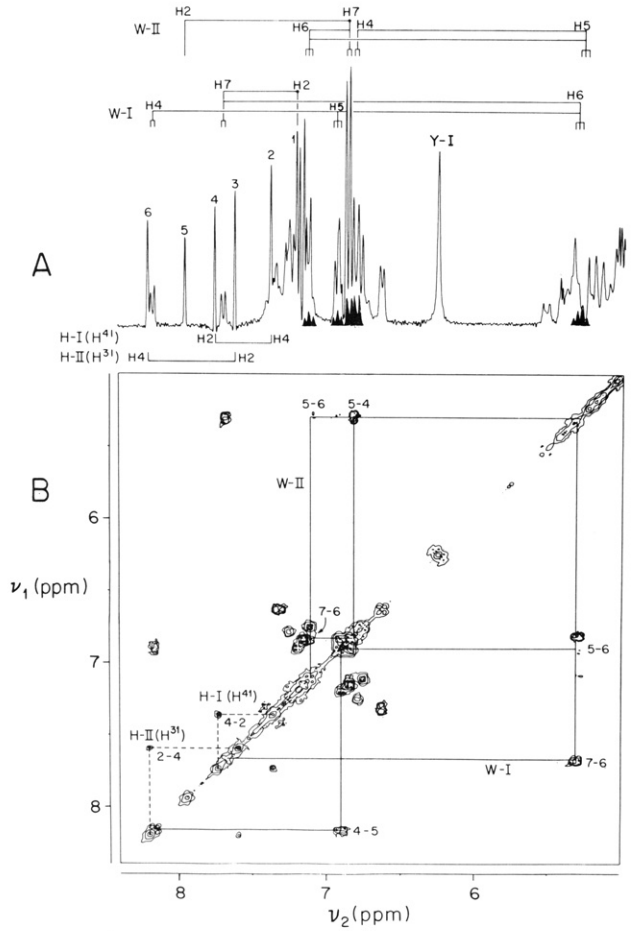

FIGURE 2: ^{1}H NMR aromatic spectra of kringle 1 at 300 MHz: identification of histidyl (H) and tryptophanyl (W) ring spin systems. *J* connectivities are indicated in the conventional 1D spectrum (A, resolution enhanced) and in the 2D COSY contour plot (B). The two-digit matrix convention is used to label cross-peaks in the COSY spectrum such that within the lower right area the first digit corresponds to the "row" proton (resonating at lower field) and the second digit corresponds to the "column" proton, namely, the coupled vicinal proton (resonating at higher field). The same cross-peak is labeled with reversed numbering in the symmetric, upper left area. Sine-bell filtering was applied in both dimensions before Fourier transformation. In the 1D spectrum (A), the Trp H2 singlets are shown connected to the corresponding H7 doublets, without implying *J* coupling between the two. His and Trp "singlets" are numbered 1–6 in (A) (De Marco et al., 1982; Motta et al., 1986). Assignment of His cross-peaks is indicated in parentheses. Unresolved Trp indole resonances are shown blackened in spectrum A, their chemical shifts being derived from the COSY spectrum (B). Kringle concentration, 5×10^{-4} M, pH* 6.7, 41 °C.

Table I: Kringle 1 Aromatic ^{1}H NMR Chemical Shifts, Resonance Assignments, and Ligand-Binding Effects[a,b]

residue (spin system)	proton	free K1 δ (ppm)	K1 + ϵACA $\Delta\delta^d$ (ppm) $\times 10^2$	K1 + BASA $\Delta\delta^d$ (ppm) $\times 10^2$
His^{33} (His-II)[c]	H2	7.59	2	−2
	H4	8.20	2	3
His^{41} (His-I)[c]	H2	7.74	−3	−7
	H4	7.36	1	−4
Phe^{36}	H2,6	6.62	11	−3
	H3,5	7.32	−5	−40
	H4	7.41	2	−21
Trp^{25} (Trp-I)[c,e]	H2	7.21	1	0
	H4	8.16	2	3
	H5	6.91	2	2
	H6	5.31	−9	−3
	H7	7.67	0	0
Trp^{62} (Trp-II)[c,e]	H2	7.82	9	10
	H4	6.82	−2	4
	H5	5.30	3	11
	H6	7.12	2	−15
	H7	6.85	−34	−61
Tyr^{-3} (Tyr-VI)	H2,6	7.16	0	−1
	H3,5	6.84	−1	0
Tyr^{9} (Tyr-V)	H2	7.26	nd[f]	nd[f]
	H3	6.72	nd	nd
	H5	6.85	nd	nd
	H6	7.19	nd	nd
Tyr^{50} (Tyr-II)	H2,6	6.92	2	−2
	H3,5	6.84	2	1
Tyr^{64} (Tyr-III)	H2,6	7.26	1	−1
	H3,5	6.78	2	0
Tyr^{72} (Tyr-I)	H2,6	6.24	19	−27
	H3,5	6.24	−7	−27
Tyr^{74} (Tyr-IV)	H2,6	7.11	3	5
	H3,5	6.75	2	5

[a] Data extracted from kringle 1 ^{1}H NMR spectra at 300 MHz, pH* ~6.75, 41 °C. [b] The identification of Phe^{36} and Tyr spin systems and their assignments supersede those given in an earlier paper (Llinás et al., 1983). [c] Assignments discussed elsewhere (Llinás et al., 1983; Motta et al., 1986). [d] $\Delta\delta > 0$ corresponds to a ligand-induced shift to low field. [e] Assignments are tentative (Llinás et al., 1985; Motta et al., 1986). [f] Not detected.

The Trp indole multiplets span the $8.2 > \delta > 5.2$ ppm region (Figure 2A,B), indicating close interactions among aromatic side chains which cause mutual ring current shifts. On the basis of the spectral analogy relating kringles 1 and 4, we have tentatively assigned Trp-I and Trp-II to Trp^{25} and Trp^{62}, respectively (Llinás et al., 1985; Motta et al., 1986). Such an assignment has received recent support from the X-ray crystallographic study of the prothrombin kringle 1 (Park & Tulinsky, 1986), since the Trp-II spectra in kringles 1 and 4 exhibit a definite pH dependence (De Marco et al., 1985b; Motta et al., 1986) and since the equivalent of the Trp^{62} side chain (Trp^{126}) is found, in the crystal structure, to be ~3.5 Å from the Ser^{121} O$^{\gamma}$, the equivalent of the plasminogen kringle's Asp^{57} γ-position. The assignments of His and Trp aromatic resonances are summarized in Table I.

Tyrosines and Phenylalanine. The Trp-II indole H2 singlet exhibits very similar low-field spectral frequencies in kringle 1 (7.82 ppm, Figure 2A) and in kringle 4 (7.80 ppm; De Marco et al., 1985b). Thus, in both proteins, the H2 resonance is significantly shifted relative to what is observed for Trp residues in small flexible peptides (7.24 ppm; Bundi & Wüthrich, 1979). This indicates that the environment surrounding the Trp^{62} indole H2 site is conserved on going from kringle 1 to kringle 4. In particular, its deshielding can only result from close interaction with an aromatic ring which, in case of the human, bovine, and porcine kringle 4, is afforded by the side chain of the site 74 residue, Tyr^{74} or Phe^{74}, depending on the homologue (Llinás et al., 1985; Trexler et al., 1985; Ramesh et al., 1986). This suggests that in kringle 1 the assignment of Tyr^{74}, a conserved residue (Figure 1), can in principle be achieved indirectly, exploiting the cross-relaxation previously observed in kringle 4 between the Tyr^{74} phenol ring and the Trp-II H2. Figure 3 shows the transient Overhauser experiment on kringle 1 at 600 MHz: irradiation of the Trp^{62} H2 singlet at 7.82 ppm elicits a response from two signals, at 7.11 and 6.76 ppm, corresponding to the AA′XX′ aromatic spin system of Tyr-IV.[2] Hence, in analogy to what is observed in kringle 4, Tyr-IV in the first kringle

[2] It should be noted that the numbering of Tyr spin systems in the kringle 1 spectrum is aimed at optimizing a matching with kringle 4 spectra and, except for Tyr-I, replaces the labels used in earlier papers (De Marco et al., 1982; Llinás et al., 1983). The latter, at any rate, need revision in view of the likely presence of extra, non-kringle 1 components which are found in samples of kringle 1 prepared by chymotryptic digestion of the kringle 1 + 2 + 3 elastase fragment under nonreducing conditions (Vâli & Patthy, 1984).

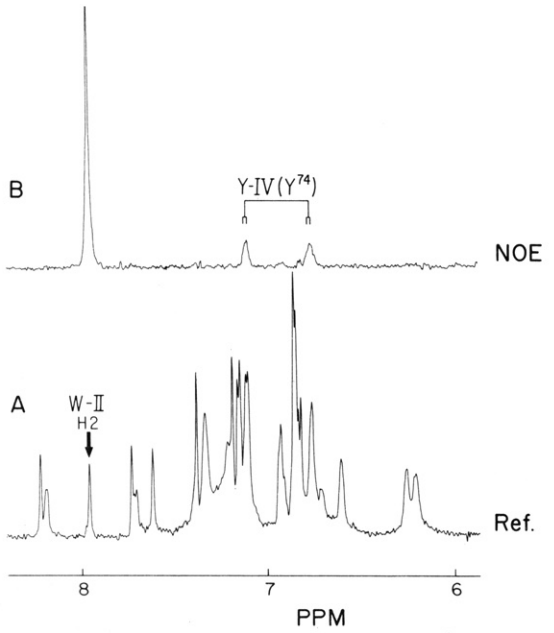

FIGURE 3: ^{1}H NMR aromatic spectra of kringle 1 at 600 MHz: transient Overhauser experiment. (A) Reference spectrum (resolution enhanced); (B) NOE difference spectrum after irradiation of the W-II (Trp^{62}) indole H2 transition, indicated by an arrow in (A), with a 25 ms radio-frequency pulse yielding 65% inversion. Perturbation of the ring proton transitions of Y-IV (Tyr^{74}) is indicated. The experiment represents 8000 scans off-resonance minus 8000 scans on-resonance, with a 250-ms NOE buildup wait before sampling; 2.6-s recycling time. Kringle concentration, 5×10^{-4} M, pH* 6.7, 24 °C.

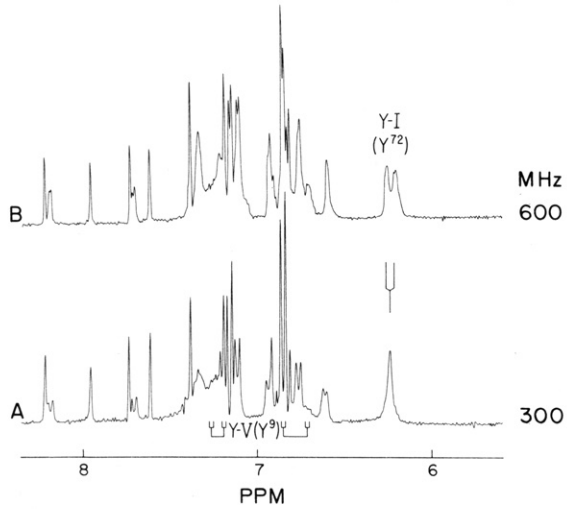

FIGURE 4: ^{1}H NMR aromatic spectra of kringle 1: effect of static magnetic field strength. The Y-I (Tyr^{72}) aromatic signal splits into two doublets on going from 300 (A) to 600 MHz (B). The Y-V ABCD resonances appear significantly broader at 300 MHz (A) than at 600 MHz (B). Kringle concentration, 5×10^{-4} M, pH* 6.7, 24 °C. Each spectrum represents an average of 1200 scans and is shown resolution enhanced.

can be confidently assigned to Tyr^{74}. Again, such an assignment is fully consistent with the crystallographic structure of the prothrombin kringle 1 (Park & Tulinsky, 1986) as it establishes a C^β to C^β distance of ~4.5 Å between the site 74 residue (Glu^{138} in the prothrombin kringle) and Trp^{62} (Trp^{126}).

Besides Tyr^{74}, kringle 1 contains five other Tyr residues located at sites −3, 9, 50, 64, and 72 (Figure 1). Except for Tyr-I, which yields a deceptive singlet at 6.24 ppm (Figure 2A), all Tyr aromatic ring protons are found to resonate between 7.4 and 6.6 ppm. Kringle 1 aromatic spectra at 300 and 600 MHz are compared in Figure 4. At 600 MHz, the

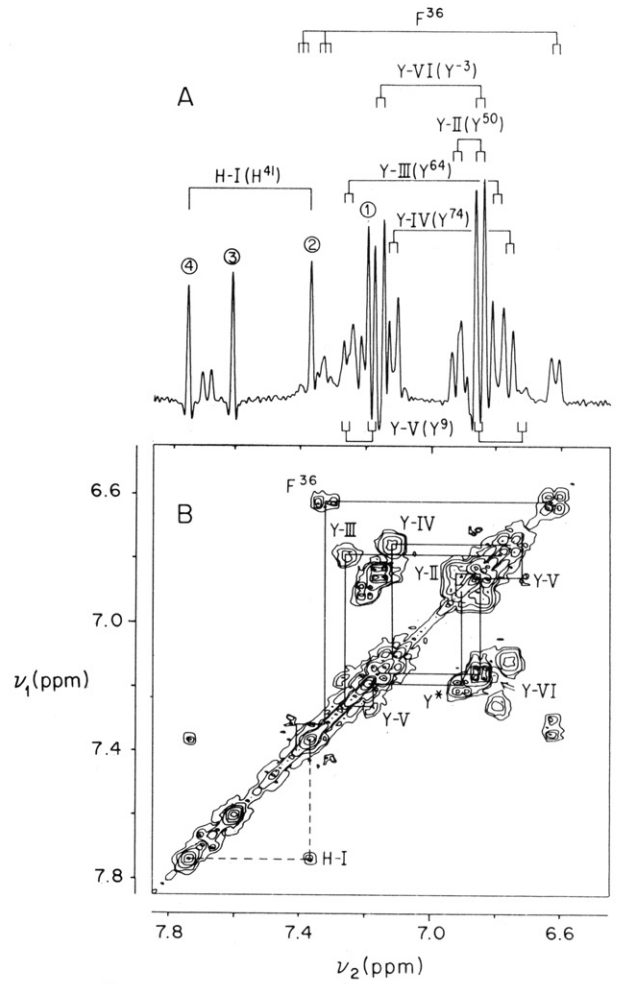

FIGURE 5: ^{1}H NMR aromatic spectra of kringle 1 at 300 MHz: identification of phenylalanyl and tyrosyl aromatic spin systems. J connectivities, indicate in the conventional 1D spectrum (A), are derived from the COSY spectrum (B). Assignments are indicated in parentheses. Circled numbers (1–4) label His and Trp singlets (see Figure 2A). An extra, unidentified Tyr connectivity is indicated Y* in the COSY spectrum B. The connectivity for H-I (His^{41}) is shown with dashed (- - -) lines. Experimental conditions are the same as for Figure 2.

Tyr-I degeneracy is removed, and two partially overlapping doublets are recovered at 6.27 and 6.21 ppm (AA′BB′ spectrum, Figure 4B), a reflection of the field/frequency dependence of the multiplet structure (Abraham, 1971). From comparisons with kringle 4, where Tyr^{72} is replaced by Trp^{72}, and from its response to BASA, Tyr-I has been assigned to Tyr^{72} (De Marco et al., 1982; Llinás et al., 1983). In kringle 5, where Tyr^{72} is conserved, a similar signal is seen at 6.3 ppm (Thewes et al., 1987).

An expansion of the aromatic 1D and 2D COSY spectra is depicted in Figure 5A and Figure 5B, respectively. The Tyr-II COSY cross-peaks lie very close to the 2D diagonal (Y-II, Figure 5B), with the AA′BB′ spectral components appearing at 6.92 and 6.84 ppm. In kringle 4 from human, porcine, and bovine plasminogens, an identical spectral pattern is observed for Tyr-II (De Marco et al., 1985b; Ramesh et al., 1986) which has been assigned to Tyr^{50} (Trexler et al., 1983, 1985). On this basis, we confidently assign Tyr-II in kringle 1 to the same conserved Tyr^{50} (Figure 1).

In analogy to what is the case for kringle 4 (De Marco et al., 1985b), magnetic field effects are manifest for the Tyr-V resonances. At 600 MHz, we observe a clear one-proton doublet at 6.72 ppm (Figure 4B) which must represent an individual Tyr-V spin as all the other aromatic one-proton

doublets (Trp indole H4 and H7 signals) have already been accounted for. While in kringle 4 the Tyr-V resonances are difficult to detect at 300 MHz (De Marco et al., 1985), in kringle 1 we observe a broad signal at 6.72 ppm (Figure 4A). As shown by the COSY spectrum, this signal is connected to a signal at 6.85 ppm (Figure 5B). The other two Tyr-V doublets are likely to be located at 7.19 and 7.26 ppm, as hinted by the cross-peaks near the diagonal in the COSY display (Figure 5B). Such a spectral pattern indicates that the Tyr-V ring is immobilized on both the 600- and 300-MHz time scales (ring flipping rate $\lesssim$300 Hz), yielding an ABCD spin system (Figure 4A,B). It also suggests that the Tyr-V side chain is somewhat more hindered in kringle 1 than in kringle 4. On the basis of its assignment in kringle 4 (Trexler et al., 1985; Ramesh et al., 1986), Tyr-V in kringle 1 is assigned to Tyr^{9}.

The sharp Tyr-VI doublets at 7.16 and 6.84 ppm (Figure 5) occur at the "random coil" positions (Bundi & Wüthrich, 1979). From acid/base titration and spin–echo experiments, we have assigned Tyr-VI, previously labeled Tyr-IV, to the N-terminal Tyr^{-3} (Motta et al., 1986). By default, Tyr-III (6.78 and 7.26 ppm) must arise from Tyr^{64}. This residue is absent in human plasminogen kringle 4, where it is replaced by Phe^{64}, but is present in kringle 5, whose Tyr-III spectral pattern (6.83 and 7.03 ppm) is closer to what we observe for the same residue in kringle 1 (T. Thewes and M. Llinás, unpublished observations).

The presence of a sixth tyrosine, yielding doublets at 7.19 and 6.90 ppm (Y* in Figure 5B), is variable. Its prominence in the 2D spectrum results from the sharpness of the resonances and is not commensurate with the level of Y* species within the sample. The COSY cross-peak is reminiscent of a similar signal observed for Tyr^{9} in kringle 4 (Esnouf et al., 1985; Ramesh et al., 1986), and that alternative assignment cannot be discarded for kringle 1.

The well-resolved two-proton doublet at 6.62 ppm (Figure 5A) is coupled to a two-proton triplet at 7.32 ppm which, in turn, is also coupled to a one-proton triplet at 7.41 ppm. Such a connectivity pattern (Figure 5B) can only originate from a Phe ring (Wider et al., 1982) and is hence assigned to Phe^{36}. The identified Phe^{36} and Tyr spin systems are indicated in Figure 5A and summarized in Table I.

Ligand Effects. While ligand binding perturbs minimally the aliphatic spectrum, significant changes are observed for the aromatic resonances. Figure 6 shows the effects of ϵACA and BASA on the aromatic 300-MHz spectrum of kringle 1. Ligand causes all His and Trp singlets to move to some extent ($0.02 \text{ ppm} < \Delta\delta < 0.04 \text{ ppm}$). Small shifts are also observed for the Trp^{25} (W-I) indole group H4 and H7 doublets at 8.16 and 7.67 ppm, respectively, and the H5 triplet at 6.91 ppm (Figure 6B). The small magnitude of these responses suggests that Trp^{25}, His^{31}, and His^{41} sense ligand presence indirectly, most likely through minor conformational rearrangements of neighboring groups with which they are in contact. Larger sensitivities to ligand binding are evidenced by the Trp^{62} (W-II) H6 triplet at 7.12 ppm, the Phe^{36} (F^{36}) H2,6 doublet at 6.62 ppm, and the Tyr^{72} (Y-I) signal at 6.24 ppm. The H6 triplet of Trp^{62} (W-II), at $\sim$7.1 ppm, is high-field-shifted by BASA ($\Delta\delta = -0.15$ ppm, Figure 6C) but is only minimally perturbed by ϵACA (Figure 6A). In contrast, the Phe^{36} (F^{36}) H2,6 doublet, at 6.62 ppm, moves to low fields when in presence of ϵACA ($\Delta\delta = 0.11$ ppm, Figure 6A) but is shifted slightly toward high fields by BASA (Figure 6C).

Most pronounced ligand effects are observed on the Tyr^{72} (Y-I) signal at 6.24 ppm (Figure 6B). Both ϵACA and BASA

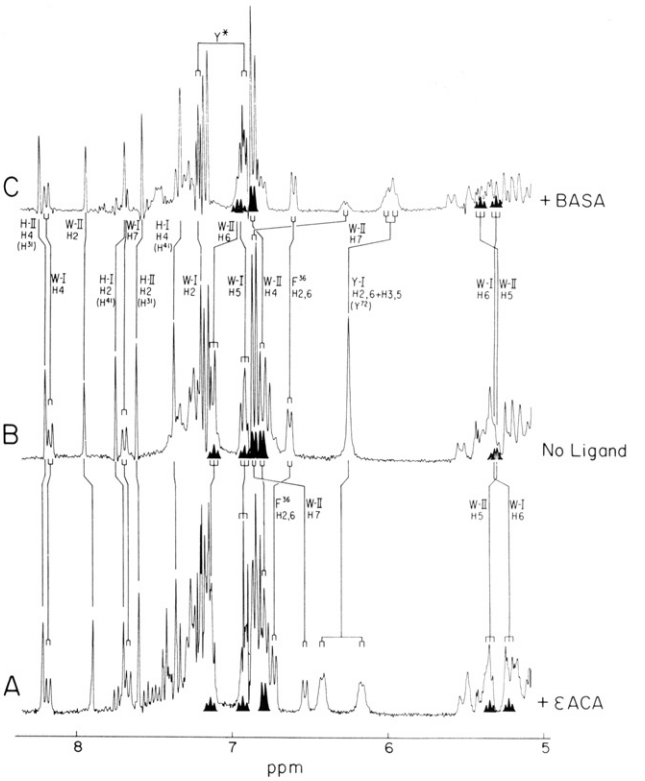

FIGURE 6: Ligand effects on the aromatic ^{1}H NMR spectrum of kringle 1 at 300 MHz, pH* 6.7, 41, °C. (A) ϵACA–kringle 1 complex; (B) ligand-free kringle 1; (C) BASA–kringle 1 complex. Kinks in the vertical line connections indicate ligand-induced shifts by reference to the free-kringle spectrum (B). Resonances discussed in the text are labeled by using the standard one-letter code for amino acid residues. Aromatic resonances are identified according to the ring proton number and their assignments are shown in parentheses. Resonances shown blackened were determined from COSY spectra. Each spectrum is the average of 2000 scans and is shown resolution enhanced. Kringle concentration, 10^{-3} M, pH* 6.7, 41 °C. Ligand levels are stoichiometric.

cause the signal to shift and resolve into two broad doublets, meaning that the ligand shifts one proton pair, H2,6 or H3,5, more or opposite relative to the other (AA′BB′ pattern, Figure 6A,C). However, the largest shift results for the Trp^{62} H7 doublet at 6.86 ppm (W-II, Figure 6B), in the presence of both ϵACA ($\Delta\delta = -0.34$ ppm, spectrum A) and BASA ($\Delta\delta = -0.61$ ppm, spectrum C). In kringle 4, where sites 62 and 72 are occupied by two Trp residues, the latters' resonances are also the most affected by BASA binding (Llinás et al., 1985; De Marco et al., 1986).

The chemical shifts of the Trp^{25} H6 and Trp^{62} H5 triplets at $\sim$5.3 ppm (W-I and W-II, Figure 6B) are conformation dependent since they resonate $\sim$−2 ppm from their random-coil positions (Bundi & Wüthrich, 1979). Such resonance frequencies are a clear indication of close interactions of the indole rings with other aromatic side chains. Figure 7 illustrates the indole doublet–triplet (H4–H5 and H7–H6) and triplet–triplet (H6–H5 and H5–H6) COSY connectivities of these resonances for the kringle ligand free (B), in the presence of ϵACA (A) and BASA (C). The perturbations—$\Delta\delta = 0.12$ ppm for the Trp^{62} H5 when in the presence of ϵACA (W-II cross peaks, Figure 7A) and $\Delta\delta = -0.09$ ppm for the Trp^{25} H6 in the presence of BASA (W-I cross-peaks, Figure 7C)—experienced by the two shifted triplets indicate a relatively larger sensitivity of the corresponding protons to ligand and suggest local conformational changes of the neighboring aromatic side chains, which are responsible for their shifted positions in the free kringle, upon ligand binding.

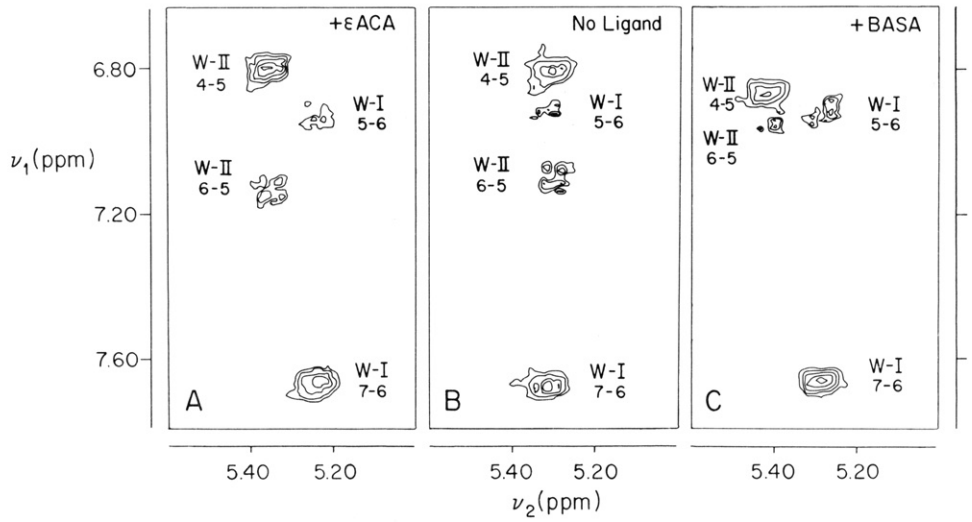

FIGURE 7: Ligand effects on the kringle 1 aromatic spectrum: Trp indole COSY cross-peak at 300 MHz. (A) εACA–kringle 1 complex; (B) ligand-free kringle 1; (C) BASA–kringle 1 complex. Cross-peaks are labeled following the two-digit matrix convention (see caption to Figure 2). Resolution enhancement in both dimensions was achieved by means of an 18°-shifted sine bell. Kringle concentration, 5×10^{-4} M; [kringle 1]/[ligand] ~ 1, pH* 6.7, 41 °C.

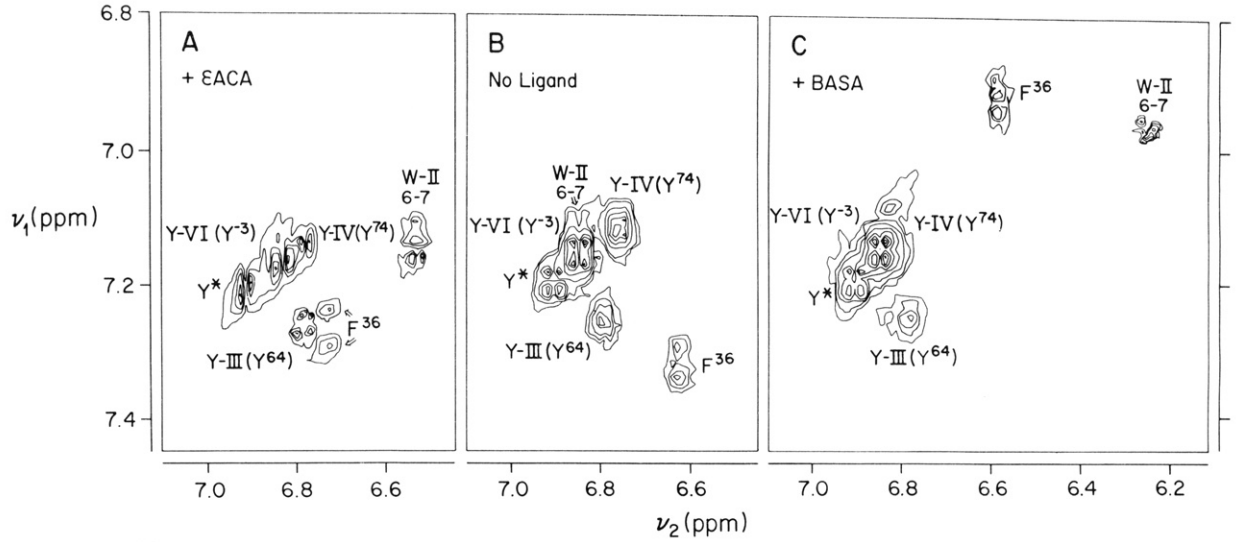

FIGURE 8: Ligand effects on the kringle 1 aromatic spectrum: COSY cross-peaks at 300 MHz. (A) εACA–kringle 1 complex; (B) ligand-free kringle 1; (C) BASA–kringle 1 complex. Contour plots B and C are shown symmetrized. Sine-bell filtering was applied to all spectra. Kringle concentration, 10^{-3} M, pH* 6.7, 41 °C. Ligand levels are stoichiometric.

Figure 8 shows the effect of ligand binding on a number of aromatic COSY cross-peaks within the spectral area 6.80 $< \delta_1 <$ 7.45 ppm and 6.50 $< \delta_2 <$ 7.10 ppm. From a comparison of spectra B with spectra A and C, it is clear that ligand binding has negligible effects on the spectra of Tyr^{64} (Y-III) or Tyr^{74} (Y-IV) which experience shifts $|\Delta\delta| < 0.05$ ppm. In contrast, significant shifts are induced on the Trp^{62} indole H7 doublet (W-II H6–H7 cross-peak) and on both the Phe^{36} ring H2,6 doublet and H3,5 triplet (F^{36}). While these results are in line with the picture provided by the 1D spectra (Figure 6), indicating a potential role for Phe^{36} and Trp^{62} in ligand binding, the data are unsupportive for a direct function for the Tyr^{64} and Tyr^{74} aromatic rings in mediating the ligand–kringle 1 interaction. Not included in Figure 8 are the cross-peaks for Tyr^{50} and Tyr^{9}, as they lie close to the COSY diagonal (Figure 3B): while Tyr^{50} is not much affected ($|\Delta\delta| \sim 0.02$ ppm), Tyr^{9} fades out from the COSY spectrum when in the presence of either ligand.

Protein–Ligand Saturation Transfer Experiments. Figure 9A shows the 300-MHz aromatic spectrum of kringle 1 in the presence of a 5-fold molar excess of BASA at pH* 6.7, 25 °C

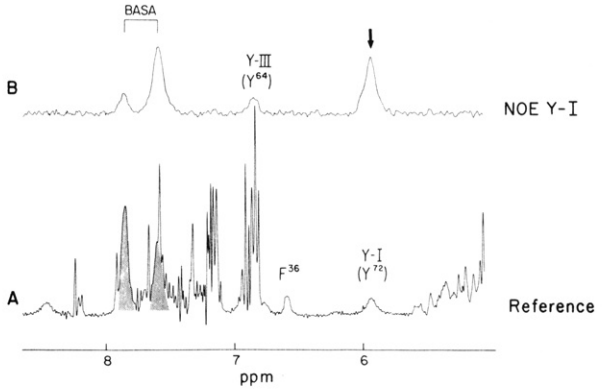

FIGURE 9: Kringle 1–BASA saturation transfer experiment at 300 MHz. (A) Reference spectrum (BASA aromatic signals are shown shaded); (B) difference spectrum upon irradiation of the Tyr^{72} aromatic transitions at 5.97 ppm (indicated by an arrow). The Tyr^{72} ring transitions were irradiated for 500 ms, using sufficient power to fully saturate the signal in about 20 ms; 2.5-s cycling time. Spectrum B represents the difference between 8000 scans off-resonance minus 8000 scans on-resonance. Spectrum A is resolution enhanced. Kringle concentration, 5×10^{-4} M, pH* 6.7, 25 °C. [Kringle 1]/[ligand] ~ 0.2.

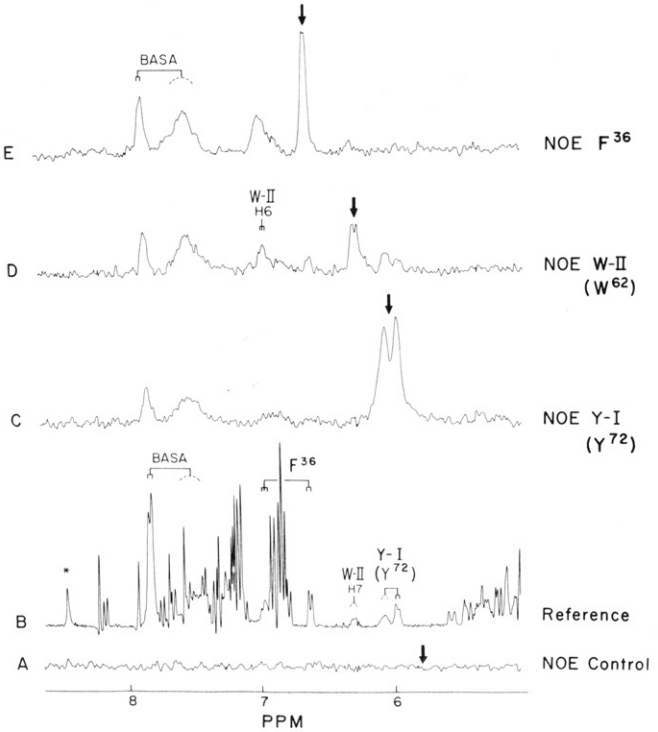

FIGURE 10: Kringle 1–BASA saturation transfer experiments at 300 MHz. (B) Kringle 1 aromatic reference spectrum; (C, D, and E) NOE difference spectra obtained by irradiating the Tyr^{72} H2,6 + H3,5, the Trp^{62} H7, and the Phe^{36} H2,6 transitions, respectively. Irradiation time, 500 ms, using sufficient power to fully saturate the signals in about 20 ms; 2.5-s cycling time. (A) Control experiment in which irradiation was applied at a blank position, indicated by the arrow, about 50-Hz high field shifted relative to the closest Tyr^{72} doublet. Kringle concentration, 5×10^{-4} M, pH* 6.7, 50 °C. [Kringle 1]/[ligand] ~ 0.2.

(ligand resonances are shown shaded). Upon irradiation of the Tyr^{72} aromatic transition(s) at 5.97 ppm, distinct effects are apparent at 7.85, 7.59, and 6.80 ppm (Figure 9B). The first two NOEs are readily identified as representing BASA signals, while the third one can be assigned to Tyr^{64}. The latter effect is in agreement with an analogous experiment on kringle 4 in which Trp^{72} was irradiated and an NOE was observed on Phe^{64} (Llinás et al., 1985).

Thus, a very efficient magnetization transfer can be established between aromatic rings from the ligand and from Tyr^{72}. Furthermore, the largest NOE is observed for the BASA meta protons, resonating at ~7.85 ppm. Considering that the NOE is inversely proportional to the sixth power of the interproton distance (Noggle & Schirmer, 1971), it can be concluded not only that the Tyr^{72} aromatic group is located close to the BASA ring but also that it interacts preferentially with the latter's H3,5 atoms.

The saturation transfer experiment described above was repeated at 50 °C (Figure 10). The Trp^{62} H7 doublet at 6.25 ppm (spectrum B), which is extremely broad at ambient temperature (Figure 9A), becomes narrowed at the higher temperature. In agreement with the experiments at 25 °C (Figure 9B), irradiation of the Tyr^{72} transitions at 5.97 ppm causes NOEs on the BASA aromatic signals at 7.85 and 7.59 ppm, with a relatively larger effect on the broad ortho signal (Figure 10B). Interestingly, the NOE at 6.80 ppm is less evident at 50 °C than at ambient temperature (Figure 9B), suggesting a dynamics-modulated interaction between the site 72 and site 64 side chains. The results shown in Figure 10C were obtained by irradiating between the two broad aromatic doublets of Tyr^{72}; however, exactly the same NOEs were

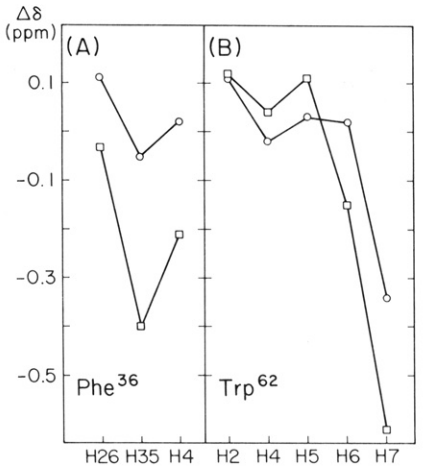

FIGURE 11: Ligand-induced shifts, $\Delta\delta$, on the Phe^{36} and Trp^{62} aromatic resonances. (A) Phe^{36}; (B) Trp^{62}; (○) ϵACA; (□) BASA. The chemical shift values were measured on COSY spectra at 300 MHz, pH* 6.7, 41 °C. $\Delta\delta > 0$ ($\Delta\delta < 0$) corresponds to a low-field (high-field) ligand-induced shift.

observed upon irradiating the individual phenol ring transitions separately (not shown).

Irradiation of the Trp^{62} ring H7 doublet at ~6.25 ppm (W-II, Figure 10D) causes the expected intraresidue effect on the indole vicinal H6 triplet at 6.97 ppm. Most interestingly, it brings about NOEs on BASA resonances as well as on the Tyr^{72} signals. Effects on BASA resonances are also elicited upon irradiation of the Phe^{36} H2,6 transition at 6.73 ppm (Figure 10E). The NOE at 6.92 ppm is an intraresidue effect on the phenyl ring H3,5 triplet. A small enhancement is also observed on the Trp^{62} indole H7 doublet.

The spectra in Figure 10D,E reveal that irradiation of the Trp^{62} H7 (W-II, spectrum D) perturbs the Phe^{36} H2,6 doublet at 6.73 ppm and the Tyr^{72} (Y-I) signals at ~5.77 ppm. Similarly, irradiation of the Phe^{36} H2,6 transitions perturbs the Trp^{62} H7 doublet (spectrum E). The selectivity of the experiments was tested by irradiating with the same radiofrequency power at a blank position, removed about 50 Hz from the highest field peak of the Tyr^{72} system (indicated by a heavy arrow in Figure 10A), which corresponds to the shortest distance between any two of the irradiated peaks. Clearly, the experiment fails to generate a detectable NOE on the aromatic resonances, confirming the specificity of the saturation transfer experiments described above.

Discussion

The aromatic ^1H NMR spectrum of kringle 1 has been fully analyzed and the resonances assigned to specific residues (Table I). The presence of aliphatic or aromatic ligands affects several of these signals (Figure 6) with the largest shifts resulting for the Phe^{36}, Trp^{62}, and Tyr^{72} ring resonances (Table I). A comparison of the effects brought about by ϵACA and BASA on Phe^{36} and Trp^{62} is shown in Figure 11, which plots $\Delta\delta$, the shifts caused by the two ligands, for the individual aromatic proton signals. Despite the different ligand structures, the curves reveal similar perturbations by the two effectors, the main difference being in the magnitude of the shifts which tend to be more pronounced in the case of BASA. This might reflect the larger size of the BASA hydrocarbon substituent or its aromatic character. However, although the chemical shifts most likely stem from a combination of factors, given their relative independence of the aliphatic/aromatic character of the ligand molecule, it would appear that local conformational rearrangements accompanying ligand binding

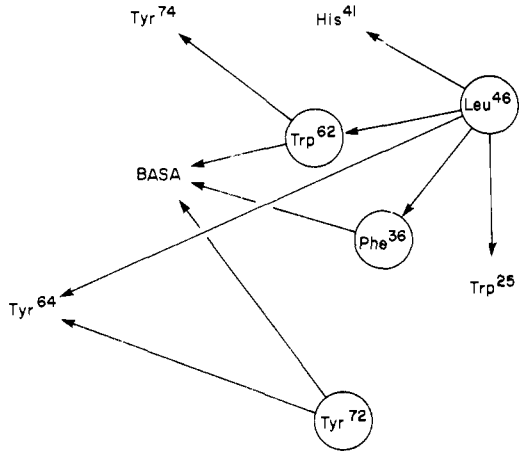

FIGURE 12: Kringle 1 NOE dipolar connectivities among residues proximal to the ligand-binding site. The connectivities are indicated by arrows that point away from the irradiated residue (within circles) toward the perturbed neighbor. Connectivities linking to BASA summarize the experimental results shown in Figures 9 and 10 while those radiating from Leu^{46} have been reported elsewhere (Motta et al., 1986). In kringle 4, the site 64 residue is known to interact with the ligand (Llinás et al., 1985).

dominate the observed effects.

Protein–ligand saturation transfer experiments (Figures 9 and 10) further assist in mapping the binding site. The combined NOE connectivity data (Figure 12) show that the ligand interacts *directly* with Phe^{36} (Figure 10E), Trp^{62} (Figure 10D), and Tyr^{72} (Figure 10C). Furthermore, mutual interactions are observed among these residues (Figure 10) and between the latter and Tyr^{64} (Figure 9B).

The requirement to include the Phe^{36} phenyl ring within the kringle 1 binding site introduces an unexpected factor for modeling the structure of the latter since, in kringle 4, site 36 is occupied by Lys^{36}, a polar residue. Indeed, for kringle 4, our modeling of the binding site thus far restricts itself to finding a satisfactory configuration for the side chains of Trp^{62}, Phe^{64}, and Trp^{72} (Llinás et al., 1985; De Marco et al., 1986; V. Ramesh et al., unpublished observations) as well as for the polar groups of Asp^{57} and Arg^{71} (Trexler et al., 1982) which define the set of side chains known to interact with the ligand. Therefore, in kringle 4, it is the central loop stretching from Cys^{51} to Cys^{75} that supports the binding site (De Marco et al., 1985a). We have not found evidence that other residues, external to this loop, play any significant direct role in the ligand–kringle 4 interaction.

It thus appears that Trp^{62} and Tyr^{72} (or Trp^{72}) afford aromatic components to the binding site in both kringle 1 and kringle 4. However, while in kringle 4 Phe^{64} is also involved, in kringle 1 we do not have evidence for a direct Tyr^{64} participation; instead, we now observe a clear contribution of Phe^{36} to ligand binding. This forces us to consider the possibility that another region of the molecule, outside the kringle central loop, is favorably disposed to interact with the ligand. This interpretation concurs with the studies of Vâli and Patthy (1984) showing that modification of Arg^{34} with 1,2-cyclohexanedione abolishes binding of ω-amino acids to kringle 1, which is most relevant as Arg^{34} immediately precedes Phe^{36} in the primary sequence (deletion at site 35, Figure 1). On the other hand, glycosylation of Asn^{34} in kringle 4 of chicken plasminogen would seem to have no effect on ligand binding (Gyenes & Patthy, 1985) which further indicates that, in contrast to what is observed for kringle 1, the area centered around site 34 in the fourth kringle is not important for binding. The combined evidence leads us to conclude that in kringle 4 the aromatic residues which interact with the ligand integrate a slightly different constellation from that found in kringle 1.

An attempt can be made to rationalize the role of Phe^{36} on the basis of the recently reported X-ray crystallographic structure of the prothrombin kringle 1 at 2.8-Å resolution (Park & Tulinsky, 1986). The prothrombin kringle, although lacking measurable lysine-binding capability, is likely to exhibit a conformation closely similar to that of the plasminogen kringles (Trexler et al., 1983; Esnouf et al., 1985). In the prothrombin homologue, the Cys^{22}-Cys^{63} loop (Cys^{87}-Cys^{127} in the prothrombin numbering) folds in such a fashion that the site 36 (site 100) side chain positions itself neighboring Trp^{62} (Trp^{126}) and Tyr^{64} (Tyr^{128}). If Ile^{100} in the prothrombin kringle is changed to a Phe residue, as found in plasminogen kringle 1, the aromatic side chain can be easily brought to interact with the ligand by torsional rotations. We therefore conclude that although the binding site is conformed by a rather fixed set of residues in both kringle 1 and kringle 4, there appears to be some flexibility, determined by the kringle folding, that enables expanding its area of definition beyond the central loop. Such a variability in the contributing aromatic sites may have a role in determining the different ligand-binding affinities of the two kringles as the association constant for various ligands is about twice as large for kringle 1 as they are for kringle 4 (Lerch et al., 1980; De Marco et al., 1982; Hochschwender et al., 1983). Furthermore, by relaxing the concept of a unique kringle binding site structure, the added flexibility of the model leads one to ponder the possibility that Asp^{55} may contribute to the anionic center provided by Asp^{57} in kringle 4 (Trexler et al., 1982) and thus play a role in ligand binding as originally suggested by Lerch and Rickli (1980). Similarly, in view of the requirement of Arg^{34} integrity for ligand binding (Vâli & Patthy, 1984), this residue too could play a similar function in kringle 1 as that assigned to Arg^{71} in kringle 4 (Trexler et al., 1982) or share with it in creating a cationic center.

In our modeling of the binding site, relevant side chains within the prothrombin kringle were substituted with those of plasminogen kringle 1, keeping the conformation of the kringle backbone and of conserved residues intact as determined crystallographically. The side chain substitutions were modeled preserving like-atom coordinates, or in their absence, in extended idealized conformations. The structure of the thusly computer-graphics-generated plasminogen kringle 1 was then modulated by torsional rotations so as to satisfy the NOE constraints. It was found that the Tyr^{74} ring could be readily positioned approximately perpendicular to the Trp^{62} indole CH2 within <4.6 Å between the methine proton and the center of the phenolic ring. Since there is an acidic (Glu^{138}) residue at site 74 in the prothrombin kringle 1, it is not surprising that the orientation of the corresponding initially modeled side chain is somewhat different in the two kringles especially given the structural relevance of ring–ring interactions among aromatic groups (Tulinsky et al., 1973; Burley & Petsko, 1985). Similarly, Phe^{36} inserted at the position of Ile^{100} in the prothrombin kringle 1 can be rotated about its χ angles so as to bring the aromatic ring close to the putative binding site. The Arg^{34} side chain was also adjusted to accommodate to the requirements of ligand binding. None of the foregoing manipulations required changes of the backbone conformation of prothrombin kringle 1.

A stereoview of the binding site area is shown in Figure 13A, which includes the substituted side chain positions prior to torsional rotations (broken) demanded by the NMR data. The

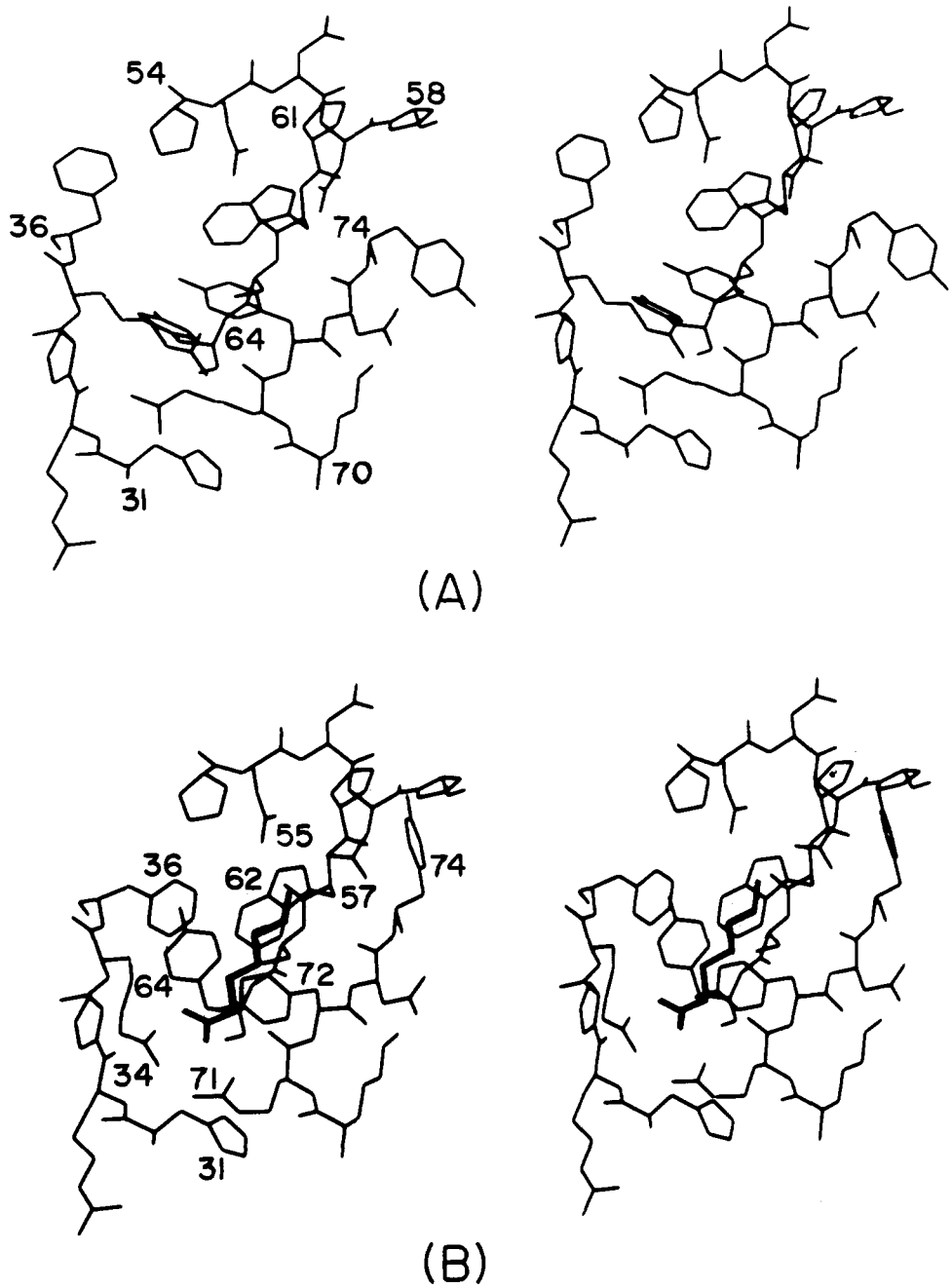

FIGURE 13: Stereoview of the plasminogen kringle 1 lysine-binding site. The model was generated from the crystallographic structure of the prothrombin kringle 1, modified to account for the ^{1}H NMR data. (A) Kringle 1 binding site; side chains are indicated before torsional displacements implemented to satisfy the NOE constraints. (B) Same as (A) but with all side chains in final position; a molecule of bound ϵACA is also included (indicated with heavy trace). Numbers label residues limiting the illustrated peptide chain segments (A) or relevant residues discussed in the text (B). Notice the absence of a site 35 residue due to deletion (Figure 1).

binding site may be described as a groove of ~8.4 Å in length by ~3.7 Å in width running diagonally in the figure. The groove is lined by the aromatic rings of Phe^{36}, Trp^{62}, and Tyr^{72}, with Tyr^{72} interacting with both Trp^{62} and, in a second plane, Tyr^{64}, a feature which explains the highly shifted position of its aromatic resonances and the observed cross-relaxation effects among these residues. One boundary is determined by the Pro^{54}-Pro^{58} pentapeptide stretch which contains both Asp^{55} and Asp^{57}. The other consists of two short, disconnected peptide segments containing Arg^{34} and Arg^{71}. The former is defined by the dipeptide Arg^{34}-Phe^{36} (residue 35 is deleted, Figure 1). In contrast to the good definition delineated by these three boundaries, the remaining boundary is ill-defined and somewhat open. In fact, this region can accommodate a polypeptide so that it is conceivably where fibrin binding occurs. The aromatic rings of His^{31}, His^{41}, and Tyr^{74} all appear around the periphery of the binding site, which explains their lesser NMR sensitivity to ligand binding. The Trp^{25} indole group (not shown) is internal to the molecule and the binding site, but nonetheless in contact with Trp^{62}.

A stereoview of the binding site with an ϵACA molecule included is shown in Figure 13B. The ligand has been positioned by assuming an extended conformation which bridges the anionic and cationic centers through ion pairing with its own, complementary polar end groups. The ligand is in intimate contact with aromatic rings on the protein surface, as evidenced by the large anisotropic NMR shifts experienced by the ligand methylene proton resonances in the complex (Motta et al., 1986). Thus, in kringle 1, the binding site appears as a well-defined area, exposing a lipophilic groove

on the surface to interact with the nonpolar moiety of the ligand while localizing the ends of the latter through two-pronged anionic and cationic centers defined by the side chain carboxylate groups of Asp^{55} and Asp^{57} on one side and conformed by the guanidino groups of Arg^{34} and Arg^{71} on the other.

In conclusion, Phe^{36} is in good contact with the Leu^{46} side chain (Figure 12) which, in conjunction with the aromatic rings of Trp^{25}, His^{41}, and Trp^{62}, contributes to the kringle hydrophobic core (Motta et al., 1986). This reinforces our model of a kernel of structural stability, centered around the Leu^{46} side chain, which is contiguous to the binding site (De Marco et al., 1985a). The latter, in turn, is expected to be endowed with ample structural flexibility and solvent exposure to allow for ligand on–off exchange between the bulk aqueous solution and the hydrophobic patch lined by the aromatic side chains which define its structure. This is consistent with a recent estimate of the ligand-binding (k_{on}) rate constant for kringle 4, which indicates that the complexation kinetics is diffusion controlled (De Marco et al., 1987) and, hence, that no significant barrier interferes with ligand access to the binding site.

References

Abraham, R. J. (1971) in *The Analysis of High Resolution NMR Spectra*, Chapter 7, Elsevier/North-Holland, New York.

Bundi, A., & Wüthrich, K. (1979) *Biopolymers 18*, 285–297.

Burley, S. K., & Petsko, G. A. (1985) *Science (Washington, D.C.) 229*, 23–28.

De Marco, A. (1977) *J. Magn. Reson. 26*, 527–528.

De Marco, A., Hochschwender, S. M., Laursen, R. A., & Llinás, M. (1982) *J. Biol. Chem. 257*, 12716–12721.

De Marco, A., Laursen, R. A., & Llinás, M. (1985a) *Biochim. Biophys. Acta 827*, 369–380.

De Marco, A., Pluck, N. D., Bányai, L., Trexler, M., Laursen, R. A., Patthy, L., Llinás, M., & Williams, R. J. P. (1985b) *Biochemistry 24*, 748–753.

De Marco, A., Laursen, R. A., & Llinás, M. (1986) *Arch. Biochem. Biophys. 224*, 727–741.

De Marco, A., Petros, A. M., Laursen, R. A., & Llinás, M. (1987) *Eur. Biophys. J. 14*, 359–368.

Dubs, A., Wagner, G., & Wüthrich, K. (1979) *Biochim. Biophys. Acta 571*, 177–194.

Ernst, R. E. (1966) *Adv. Magn. Reson. 2*, 1–135.

Esnouf, P., Lawerence, M. P., Mabbutt, B. C., Patthy, L., Pluck, N., & Williams, R. J. P. (1985) *Bull. Soc. Chim. Belg. 94*, 883–896.

Ferrige, A. G., & Lindon, J. C. (1978) *J. Magn. Reson. 31*, 337–340.

Gordon, S. L., & Wüthrich, K. (1978) *J. Am. Chem. Soc. 100*, 7094–7098.

Gyenes, M., & Patthy, L. (1985) *Biochim. Biophys. Acta 832*, 326–330.

Hochschwender, S. M., Laursen, R. A., De Marco, A., & Llinás, M. (1983) *Arch. Biochem. Biophys. 223*, 58–67.

Jones, T. A. (1982) in *Computational Crystallography* (Sayer, D., Ed.) pp 303–317, Clarendon Press, Oxford.

Lerch, P. G., & Rickli, E. E. (1980) *Biochim. Biophys. Acta 625*, 374–378.

Lerch, P. G., Rickli, E. E., Lergier, W., & Gillessen, D. (1980) *Eur. J. Biochem. 107*, 7–13.

Llinás, M., De Marco, A., Hochschwender, S. M., & Laursen, R. A. (1983) *Eur. J. Biochem. 135*, 379–391.

Llinás, M., Motta, A., De Marco, A., & Laursen, R. A. (1985) *J. Biosci. 8*, 121–139.

Motta, A., Laursen, R. A., Rajan, N., & Llinás, M. (1986) *J. Biol. Chem. 261*, 13684–13692.

Noggle, J. H., & Schirmer, R. E. (1971) *The Nuclear Overhauser Effect: Chemical Applications*, Academic Press, New York.

Park, C. H., & Tulinsky, A. (1986) *Biochemistry 25*, 3977–3982.

Ramesh, V., Gyenes, M., Patthy, L., & Llinás, M. (1986) *Eur. J. Biochem. 159*, 581–595.

Sottrup-Jensen, L., Claeys, H., Zajdel, M., Petersen, T. E., & Magnusson, S. (1978) *Prog. Chem. Fibrinolysis Thrombolysis 3*, 191–209.

Szevereneyi, N. M., Bothner-By, A. A., & Bittner, R. (1980) *J. Phys. Chem. 84*, 2880–2883.

Thewes, T., Ramesh, V., Simplaceanu, E. L., & Llinás, M. (1987) *Biochim. Biophys. Acta 912*, 254–269.

Thorsen, S., Clemmensen, I., Sottrup-Jensen, L., & Magnusson, S. (1981) *Biochim. Biophys. Acta 668*, 377–387.

Trexler, M., Váli, Z., & Patthy, L. (1982) *J. Biol. Chem. 257*, 7401–7406.

Trexler, M., Bányai, L., Patthy, L., Pluck, N. D., & Williams, R. J. P. (1983) *FEBS Lett. 154*, 311–318.

Trexler, M., Bányai, L., Patthy, L., Pluck, N. D., & Williams, R. J. P. (1985) *Eur. J. Biochem. 152*, 439–446.

Tulinsky, A., Vandlen, R. L., Morimoto, C. N., Mani, N. V., & Wright, L. H. (1973) *Biochemistry 12*, 4185–4192.

Váli, Z., & Patthy, L. (1984) *J. Biol. Chem. 259*, 13690–13694.

Wider, G., Lee, K. H., & Wüthrich, K. (1982) *J. Mol. Biol. 155*, 367–388.

Wider, G., Macura, S., Kumar, A., Ernst, R. R., & Wüthrich, K. (1984) *J. Magn. Reson. 56*, 207–234.

Wiman, B., Lijnen, H. R., & Collen, D. (1979) *Biochim. Biophys. Acta 579*, 142–154.